

# Analytical Methods

Accepted Manuscript



This is an *Accepted Manuscript*, which has been through the Royal Society of Chemistry peer review process and has been accepted for publication.

*Accepted Manuscripts* are published online shortly after acceptance, before technical editing, formatting and proof reading. Using this free service, authors can make their results available to the community, in citable form, before we publish the edited article. We will replace this *Accepted Manuscript* with the edited and formatted *Advance Article* as soon as it is available.

You can find more information about *Accepted Manuscripts* in the [Information for Authors](#).

Please note that technical editing may introduce minor changes to the text and/or graphics, which may alter content. The journal's standard [Terms & Conditions](#) and the [Ethical guidelines](#) still apply. In no event shall the Royal Society of Chemistry be held responsible for any errors or omissions in this *Accepted Manuscript* or any consequences arising from the use of any information it contains.

**A New Fluorescent Rhodamine B Derivative as “Off-On”  
Chemosensor for Cu<sup>2+</sup> with High Selectivity and Sensitivity**

Xianfu Meng, Yanxia Xu, Jinliang Liu\*, Lining Sun, and Liyi Shi\*

*Research Center of Nano Science and Technology, Shanghai University, 200444, China.*

\* To whom correspondence should be addressed:

Assoc. Prof. Jinliang Liu

Research Center of Nano Science and Technology,

Shanghai University, 200444, China.

Telephone: +86-21-66137197

Fax: +86-21-66137197

Email: [liujl@shu.edu.cn](mailto:liujl@shu.edu.cn)

Prof. Liyi Shi

Research Center of Nano Science and Technology,

Shanghai University, 200444, China.

Email: [shiliyi@shu.edu.cn](mailto:shiliyi@shu.edu.cn).

## Abstract

A novel fluorescence chemosensor containing two rhodamine B moieties per molecule was synthesized and characterized as an “off-on” fluorescent probe for the detection of copper ions ( $\text{Cu}^{2+}$ ). The crystal structure of the chemosensor was confirmed by X-ray analysis and the recognition mechanism of detecting  $\text{Cu}^{2+}$  was proposed with the absorption and fluorescence characterization. The chemosensor showed high selectivity and sensitivity and good repetition in sensing  $\text{Cu}^{2+}$ , and the detection limit is as low as 38.00 nM. In addition, the chemosensor displayed low cytotoxicity as revealed by methyl thiazolyl tetrazolium (MTT) assays and was successfully applied to fluorescence test paper and living cell imaging for detecting  $\text{Cu}^{2+}$ . Therefore, based on being environment friendly and good biocompatibility, the results offered the advantages including the detection of  $\text{Cu}^{2+}$  in environment and bioimaging of intracellular  $\text{Cu}^{2+}$ .

**Keywords:** Fluorescence chemosensor; Cell imaging; Rhodamine B derivative

## 1. Introduction

Recently, more and more interests have been attracted on detecting copper ions ( $\text{Cu}^{2+}$ ) because  $\text{Cu}^{2+}$  is indispensable during many fundamental processes in human beings and environmental cycle as well.<sup>1-7</sup>  $\text{Cu}^{2+}$  is highly toxic when it is of high concentration in human body, leading to several serious diseases, such as Menkes, Wilson and Alzheimer.<sup>8-14</sup> It can also cause infant liver damage<sup>15, 16</sup> as well as childhood cirrhosis<sup>17</sup> when it is accumulated more in the body. Up to now, considerable efforts have been devoted to developing efficient methods to detect and trace  $\text{Cu}^{2+}$ , such as, atomic absorption spectrometry, inductively coupled plasma atomic emission spectrometry (ICP-AES), and inductively coupled plasma mass spectroscopy (ICP-MS), and so on.<sup>18-23</sup> Among these approaches, fluorescent probes have been recently considered as a promising candidate owing to the virtues of easy operation, high sensitivity, rapid response and non-destructive sensing characteristics.<sup>17, 24-28</sup> However, due to the paramagnetic nature of copper ions, most of the  $\text{Cu}^{2+}$  fluorescent probes reported often show “on-off” signals upon the bonding of  $\text{Cu}^{2+}$ . These probes are not fit for analytical application because the quenching of the fluorescence may be caused by other quenchers and false results may be obtained by using this kind of probe for  $\text{Cu}^{2+}$  detection.<sup>29-34</sup>

On the contrary, introducing rhodamine moiety to construct “off-on” probes is an ideal alternative approach due to the well-known spirolactam (fluorescence off) to ring-opened amide (fluorescence on) equilibrium of rhodamine derivatives.<sup>35-40</sup> Owing to the excellent photophysical properties, such as high absorptivity, excellent fluorescence quantum yield and good photostability, rhodamine derivative has become one of the most popular fluorescent probes for the construction of artificial fluorescent probes.<sup>41, 42</sup> Furthermore, based on the Soft-Hard Acid-Base principle, the probes that contain the recognition moiety with O and N atoms could exhibit good affinity to  $\text{Cu}^{2+}$ .

In this work, a novel fluorescent chemosensor containing two rhodamine B moieties per molecule was synthesized by using 3-di-(formaldehyde phenoxy)-2-propanol (denoted as DFPP) and rhodamine B hydrazide (denoted as RhB-NH<sub>2</sub>) through a convenient Schiff base reaction. The obtained Rhodamine B derivative (denoted as DFPP-RhB) was characterized and investigated to be an “off-on” fluorescent probe for the detection of Cu<sup>2+</sup> with high selectivity and sensitivity. In addition, the chemosensor displayed low cytotoxicity as revealed by methyl thiazolyl tetrazolium (MTT) assays and was successfully applied to fluorescence test paper and living cell imaging for detecting Cu<sup>2+</sup>. Therefore, based on being environment friendly and good biocompatibility, the results offered the advantages including the detection of Cu<sup>2+</sup> in environment and bioimaging of intracellular Cu<sup>2+</sup>.

## 2. Experimental section

### 2.1 Chemicals

Hydrazine hydrate (85%) and Rhodamine B were purchased from J&K Chemical Ltd. salicylaldehyde was bought from Aladdin. All other chemicals were purchased from Sinopharm Chemical Reagent Co. Ltd and used as received. The solutions of metal ions including Cu<sup>2+</sup>, Mg<sup>2+</sup>, Ba<sup>2+</sup>, Mn<sup>2+</sup>, Zn<sup>2+</sup>, Li<sup>+</sup>, Na<sup>+</sup>, K<sup>+</sup>, Ca<sup>2+</sup>, Hg<sup>2+</sup> used in this paper were prepared in deionized water from their chloride salts, except that the solution of Co<sup>2+</sup> was prepared from Co(NO<sub>3</sub>)<sub>2</sub>.

### 2.2 Characterization

<sup>1</sup>H NMR and <sup>13</sup>C NMR spectra were performed on an AVANCE 500 MHz spectrometer, using tetramethylsilane (TMS) as an internal standard. Electrospray ionization mass spectrometry (ESI-MS) spectra were obtained on a Micromass LCTTM mass spectrometer. UV-Vis spectra were recorded on a 760CRT dual beam spectrophotometer. Fluorescence spectra were determined on a LS-55 spectrophotometer with 10 nm excitation slit and 7.5 nm emission one. The excitations

wavelengths were 520 nm, and the emissions were collected from 530 to 700 nm. All the measurements mentioned above were conducted at room temperature (about 298K).

### 2.3 The analysis of X-ray crystallography

The crystals were obtained by diffusing petroleum ether slowly into a solution of DFPP-RhB in dichloromethane. An appropriate single crystal was coated in a glass fiber, and cooled fast under low-temperature nitrogen environment, and then, diffraction measurements were collected on a Bruker APEXII DUO (two light source) X-ray diffractometer with Mo K $\alpha$  graphite monochromated radiation. The crystal structures were solved by direct methods using SHELXS-97 software and refined on F<sup>2</sup> by using SHELXS-97 program incorporated in SHELXS software package. The refinement and all future calculations were carried out using SHELXS-97.<sup>43, 44</sup> The non-H atoms were refined anisotropically, using weighted full matrix least-squares on F<sup>2</sup>. What's more, the hydrogen atoms were included in the models in calculated positions and were refined as constrained to bonding atoms for DFPP-RhB.

### 2.4 Synthesis

The detailed synthetic procedure of DFPP-RhB was shown in Scheme S1.

#### 2.4.1 Synthesis of 1, 3-di-( formaldehyde phenoxy)-2-propanol

1, 3-di-(formaldehyde phenoxy)-2-propanol (DFPP) was synthesized according to a previous literature.<sup>45</sup> <sup>1</sup>H NMR (DMSO-d<sub>6</sub>),  $\delta$ (ppm) : 10.40 (s, 2H, CHO) ; 6.92-7.69 (m, 8H, ArH); 4.30-4.54 (m, 5H, CH<sub>2</sub>CHCH<sub>2</sub>); 3.35 (br, 1H, OH).

#### 2.4.2 Synthesis of Rhodamine B hydrazide

Rhodamine B hydrazide (RhB-NH<sub>2</sub>) was synthesized according to a previous report with some modification<sup>35</sup> : in a 100 mL of two-neck flask, rhodamine B (4.791g, 10 mmol) was added and dissolved in 30 mL of ethanol. 12 mL (excessive) of hydrazine hydrate (85%) was added dropwise

into the flask with stirring vigorously at room temperature. After that, the mixture was heated to reflux in an Ar bath for 8 hours. After cooling, the solvent was removed under reduced pressure. The precipitate was washed by deionized water and dried under reduced pressure. **<sup>1</sup>H NMR (DMSO-d<sub>6</sub>) δ (ppm):** 7.77 (m, 1H, ArH), 7.45 (m, 2H, ArH), 7.03(m, 1H, ArH) , 6.38 (s, 2H, xanthene-H) , 6.33(s, 4H, xanthene-H), 3.38(s, 2H, NH<sub>2</sub>), 3.31(q, 8H, NCH<sub>2</sub>CH<sub>3</sub>), 1.09(t, 12H, NCH<sub>2</sub>CH<sub>3</sub>).

### 2.4.3 Synthesis of DFPP-RhB

0.687 g of RhB-NH<sub>2</sub> (1.5 mmol) was dissolved in 15 mL of ethanol. Then 0.144 g (0.5 mmol) of DFPP dissolved in 15 mL of ethanol was added dropwise with vigorous stirring. The mixture was heated to reflux in an Ar bath for 8 hours. The precipitate was obtained under reduced pressure, washed 3 times by cold ethanol and dried in vacuum. The crude product was purified by silica gel column chromatography using petroleum ether/ethyl acetate (1:2, v/v) as eluent. **<sup>1</sup>H NMR (DMSO-d<sub>6</sub>) δ (ppm):** 9.14 (s, 2H, N=C-H), 7.90 (d, 2H, ArH, J=6.0 Hz), 7.57 (m, 6H, ArH), 7.29 (m, 2H, ArH), 6.99 (t, 2H, ArH, J<sub>ac</sub>=14.6 Hz), 6.29-6.50 (m, 12H, ArH), 4.30-4.54 (m, 5H, CH<sub>2</sub>CHCH<sub>2</sub>), 3.35 (s, 1H, OH), 3.23 (q, 16H, NCH<sub>2</sub>CH<sub>3</sub>), 1.09 (t, 24H, NCH<sub>2</sub>CH<sub>3</sub>, J<sub>ac</sub>=13.05). **<sup>13</sup>C-NMR (DMSO-d<sub>6</sub>) δ (ppm):** 12.85, 44.05, 65.70, 67.89, 69.65, 97.85, 105.84, 113.29, 121.21, 124.17, 127.96, 131.98, 134.21, 143.54, 148.88, 151.93, 153.02, 157.46, 164.19. **MS (ESI) m/z:** [M+H]<sup>+</sup>: 1177.5.

### 2.5 Metal-ions Sensing procedures

A stock solution of DFPP-RhB (10 μM) was prepared in absolute ethyl alcohol. Stock solutions of the metal ions (0.1 M) were prepared in deionized water. Titration experiments were performed by adding Cu<sup>2+</sup> stock solution incrementally to a solution of DFPP-RhB (2.5 mL) by means of a micro-pipette. For the selectivity experiments, the test samples were prepared by adding

appropriate amounts (100 equiv.) of metal ions solution to 2.5 mL of a solution of DFPP-RhB (10  $\mu$ M). In competition experiments,  $\text{Cu}^{2+}$  was added to the solutions containing DFPP-RhB and other metal ions of interest. All solutions were stirred for 1 min at room temperature and then used for the spectroscopic test. For fluorescence measurements, excitation and emission slit widths were 3 nm and 5 nm, respectively. Excitation was provided at 525 nm, and emission was collected from 535 nm to 700 nm.

2.6 Cell culture

Human cervical carcinoma HeLa cells were provided by the Institute of Biochemistry and Cell Biology for Biological Sciences (SIBS), Chinese Academy of Sciences (CAS) (China). The HeLa cells were grown in Dulbecco's modified Eagle's medium (DMEM) supplemented with 10% Fetal Bovine Serum (FBS) at 37 °C and 5%  $\text{CO}_2$ .

2.7 Cytotoxicity test *in vitro*

The *in vitro* cytotoxicity of DFPP-RhB was estimated by performing methyl thiazolyl tetrazolium (MTT) assays on the HeLa cells. Cells were seeded in a 96-well plate at  $1 \times 10^4$ /well under 100 % humidity, and allowed to adhere for 24 h at 37 °C and 5%  $\text{CO}_2$ . Then, different concentration of DFPP-RhB (0~50  $\mu$ M) were added to the wells, and the cells were subsequently incubated for additional 24 h at 37 °C under 5%  $\text{CO}_2$ . The combined MTT/phosphate buffered solution (PBS) solution was added to each well of the 96-well assay plate, and incubated for an additional 4 h in the same conditions. Cells treated with serum free media were considered as control group. An enzyme-linked immunosorbent assay (ELISA) reader (infinite M200, Tecan, Austria) was used to measure the OD570 (Absorbance value) of each well referenced at 490 nm. The following formula was used to calculate the viability of cell growth:

Viability (%) = (mean of Absorbance value of treatment group/mean Absorbance value of



control)  $\times 100$ .

## 2.8 Fluorescence imaging

The cells were washed with PBS before the experiments, and then incubated with  $10\ \mu\text{M}\ \text{Cu}^{2+}$  for 0.5 h at  $37\ ^\circ\text{C}$ . After that, the cells were incubated with  $10\ \mu\text{M}\ \text{DFPP-RhB}$  in DMSO/PBS (pH 7.4, 1:99, v/v) for 0.5 h at  $37\ ^\circ\text{C}$ . After washing the cells with PBS, cell imaging was implemented. The fluorescence imaging was performed with an Olympus FluoView FV1000 confocal fluorescence microscope and a 60 oil-immersion objective lens. Cells incubated with DFPP-RhB were excited at 543 nm with a HeNe laser, and the emission was collected at  $580 \pm 20\ \text{nm}$ .

## 3. Results and discussion

### 3.1 Synthesis and characterization of DFPP-RhB

The fluorescence chemosensor DFPP-RhB was synthesized via a Schiff base reaction from 3-di-(formaldehyde phenoxy)-2-propanol and rhodamine B hydrazide (Scheme S1, Supporting Information) and its structure was confirmed by using  $^1\text{H}$  NMR (Fig. S1, Supporting Information),  $^{13}\text{C}$  NMR and ESI-MS spectra. The structure of DFPP-RhB, with the numbering scheme, is displayed in Fig. 1. From the crystalline picture, we can see that this novel chemosensor contains two rhodamine B moieties per molecule with a symmetrical configuration. Crystallographic data for DFPP-RhB are listed in Table S1 and Table S2 (Supporting Information). The two imine bonds are N(2)-C(9) and N(6)-C(45), and the bond lengths of them are  $1.283\ \text{\AA}$  and  $1.274\ \text{\AA}$ , respectively, which is similar to the result reported by Xu et al.<sup>46,47</sup> The crystallographic result can demonstrate the formation of imine group in the chemosensor molecule, which is expected to chelate with copper ions by the imino N<sup>48</sup> together with the carbonyl O.

### 3.2 Spectra response of DFPP-RhB towards metal ions

Rhodamine B hydrazide can be used as the fluorescent probe for soft metal ions because of the

well-known equilibrium between the non-fluorescent spirolactam and the fluorescent ring-opened amide of rhodamine. The UV-Vis and fluorescence spectra of DFPP-RhB towards various metal ions are illustrated in Fig. 2A and Fig. 2B, respectively. Upon the addition of  $\text{Cu}^{2+}$ , significant enhancements in UV-Vis absorption at 552 nm (almost 100-fold) and fluorescence intensity at 580 nm (almost 40 fold) can be observed, indicating a  $\text{Cu}^{2+}$ -induced ring opening reaction of the spirolactam form has happened in the rhodamine unit of the synthesized DFPP-RhB. The absorption and fluorescence spectra were almost no changed upon the introduction of other metal ions, including  $\text{Mg}^{2+}$ ,  $\text{Co}^{2+}$ ,  $\text{Ba}^{2+}$ ,  $\text{Mn}^{2+}$ ,  $\text{Zn}^{2+}$ ,  $\text{Li}^{+}$ ,  $\text{Na}^{+}$ ,  $\text{K}^{+}$  and  $\text{Ca}^{2+}$ , even  $\text{Hg}^{2+}$  which was often thought of as the most interferential ion to  $\text{Cu}^{2+}$ ,<sup>38, 49-51</sup> indicating that this chemosensor detects  $\text{Cu}^{2+}$  exclusively over other metal ions. Correspondingly, as shown in Fig. 2C and Fig. 2D, a solution of DFPP-RhB in ethanol is colorless and non-fluorescence, indicating that the spirocyclic form is retained. Upon the addition of  $\text{Cu}^{2+}$  into the ethanol solution of DFPP-RhB, a color change from colorless to purple is observed immediately, and a significant fluorescence enhancement occurs as well. Neither color change nor fluorescence enhancement was observed in the selective experiments using other metal ions under the identical condition indicating that this chemosensor could be served as a sensitive “naked-eye” chemosensor for  $\text{Cu}^{2+}$ . Additionally, competition experiments were further carried out by adding  $\text{Cu}^{2+}$  to the solutions containing both DFPP-RhB and the metal ions of interest. As shown in Fig. S2 (Supporting Information), these co-existent ions had negligible interference on  $\text{Cu}^{2+}$  sensing even the competitive ions were present at high concentrations.

The detailed titration experiments of DFPP-RhB upon varying amounts of  $\text{Cu}^{2+}$  (0-400  $\mu\text{M}$ ) in ethanol solutions were performed and the changes in absorption spectra is shown in Fig. 3A. Upon the addition of  $\text{Cu}^{2+}$  gradually, an absorption band centered at 552 nm appears and the intensity increases evidently, indicating the undergoing of the ring-open process of the rhodamine B unit in

DFPP-RhB. A linear increase of the absorbance intensity can be observed with the increasing of  $\text{Cu}^{2+}$  in a wide range from 0 to 10  $\mu\text{M}$  (Inset of Fig. 3A). The reaction reached saturation with a 100-fold increase of absorbance when 8 equiv.  $\text{Cu}^{2+}$  was added. According to the formula  $\text{LOD}=3S_0/S$  (where 3 is the factor at the 99% confidence level,  $S_0$  the standard deviation of the blank measurements, and  $S$  is the slope of the calibration curve). As shown in Fig.4, the detection limit (LOD) of the chemosensor towards  $\text{Cu}^{2+}$  was calculated to be 38.00 nM, suggesting the high sensitivity of the chemosensor for detecting  $\text{Cu}^{2+}$ . Similarly, as shown in the fluorescence titration spectra (Fig. 3B), a linear increase of fluorescence intensity could be observed as well with the increasing of  $\text{Cu}^{2+}$  concentration over a wide range, and the LOD was calculated to be 0.58  $\mu\text{M}$  based on the fluorescence technique. It must be pointed out that a continuous red shift of the emission peak from 573 to 585 nm was obtained, and this sensing result was similar to that of the probe synthesized by Tong et al.<sup>37</sup>

Based on the high selectivity and sensitivity of DFPP-RhB towards  $\text{Cu}^{2+}$  mentioned above, the test paper with DFPP-RhB was prepared to be used to detect  $\text{Cu}^{2+}$ . As shown in Fig. S3 in the supporting information, the test paper was colorless and non-fluorescence. Upon the addition of  $\text{Cu}^{2+}$ , a color change from colorless to purple occurred immediately, and a significant fluorescence could be observed under excitation with UV light at 365 nm. Therefore the obtained test paper provides a convenient method to detect  $\text{Cu}^{2+}$  easily by using naked-eyes.

### 3.3 Recognition mechanism of DFPP-RhB towards $\text{Cu}^{2+}$

To understand the probable recognition mechanism of DFPP-RhB towards  $\text{Cu}^{2+}$ , the method of continuous variations (Job's plot) was conducted from the DFPP-RhB- $\text{Cu}^{2+}$  system in ethanol solution. The Job's plot (Fig. S4, Supporting Information) clearly demonstrated a 1:1 stoichiometry between DFPP-RhB and  $\text{Cu}^{2+}$ . Furthermore, the ESI-MS of DFPP-RhB and DFPP-RhB- $\text{Cu}^{2+}$

complex shown in Fig. S5 can also suggest the 1:1 stoichiometry mentioned above. As shown in the top spectrum of the figure, the peak at  $m/z=1177.5$  was resulted from the  $[DFPP-RhB-H^+]$ , while, after the addition of excessive  $Cu^{2+}$  (20 equiv) to the solution, a unique peak at  $m/z=1241.4$  corresponding to  $[DFPP-RhB-Cu^{2+}-H^+]$  appeared (Fig. S5C, Supporting Information), which demonstrated the formation of a 1:1 stoichiometry mode. Furthermore, from the nonlinear fitting of the titration curve, we assumed a 1:1 stoichiometry for DFPP-RhB- $Cu^{2+}$  complex (Fig. 5), with an association constant  $K_a$  value of  $6.67 \times 10^5$ ,<sup>52-54</sup> which showed the high affinity of DFPP-RhB to  $Cu^{2+}$ . Furthermore, the reversible behavior of DFPP-RhB upon  $Cu^{2+}$  was conducted by adding EDTA (10 equiv) aqueous solution to the solution of DFPP-RhB containing  $Cu^{2+}$ . After the addition of EDTA aqueous solution the color of the solution of DFPP-RhB containing  $Cu^{2+}$  changed from purple to colorless immediately, and at the same time, the UV-Vis absorption at 552 nm decreased significantly. In addition, the relative quantum yields of the chemosensor after interaction with  $Cu^{2+}$  was calculated to be 7.87% (Fig. S6, Supporting Information).

### 3.4 Fluorescence bioimaging of intracellular $Cu^{2+}$

To investigate the potential biological application of chemosensor DFPP-RhB, the biocompatibility is essential to evaluate and the methyl thiazolyl tetrazolium (MTT) assay was employed to study its cytotoxicity (Fig. S7, Supporting Information). Assuming that the viability of untreated HeLa cells was 100%, the viabilities of the cells incubated with different concentrations of DFPP-RhB for 24 h at 37 °C were estimated to be higher than 95%, even at a relatively high concentration of 50  $\mu$ M. The MTT assay results demonstrated that the synthesized chemosensor has low cytotoxicity and good biocompatibility in the dosages range studied and can be served as a potential probe for living cell imaging.

Based on the excellent detection property of DFPP-RhB upon  $Cu^{2+}$ , confocal microscopy

experiments were carried out to display its applicability in bioimaging of intracellular  $\text{Cu}^{2+}$ . As determined by laser scanning confocal microscopy, the HeLa cells show no intracellular fluorescence after being incubated with 10  $\mu\text{M}$  of DFPP-RhB for 0.5 h at 37  $^{\circ}\text{C}$ , (Fig. 6, the top three pictures). When the cells were supplemented with 10  $\mu\text{M}$   $\text{Cu}^{2+}$  in the medium for 0.5 h at 37  $^{\circ}\text{C}$  and then incubated with DFPP-RhB under the same condition, a significant fluorescence increase was observed from the intracellular region (Fig. 6, the bottom three pictures). From the brightfield measurements with or without the treatment with  $\text{Cu}^{2+}$ , it could be noted that the cells were viable throughout the imaging experiments. The overlay of brightfield and fluorescence pictures indicated the fluorescence signals were localized around the cytosol region rather than merely staining the membrane surface. These results demonstrated that the chemosensor could be used for monitoring subcellular distribution of  $\text{Cu}^{2+}$  in biological samples.

## Conclusions

In summary, a new “off-on” fluorescence chemosensor DFPP-RhB which specifically responds to  $\text{Cu}^{2+}$  has been successfully prepared by using a simple method. The chemosensor DFPP-RhB shows high selectivity and sensitivity and good repetition for the detection of  $\text{Cu}^{2+}$ . And the detection of limit is as low as 38.00 nM. The crystal structure of DFPP-RhB has been confirmed and the recognition mechanism of detecting  $\text{Cu}^{2+}$  was proposed. With the good emission property of DFPP-RhB- $\text{Cu}^{2+}$  complex and good biocompatibility of DFPP-RhB, the chemosensor was successfully applied to fluorescence test paper and living cell imaging for detecting  $\text{Cu}^{2+}$ . Therefore we hope this chemosensor could play an important role in physiology and pathology science in the future.

## Acknowledgment

We are grateful for the financial support from the National Natural Science Foundation of China

(Grant Nos. 21201117, 21231004), and State Key Laboratory of Pollution Control and Resource Reuse Foundation (NO. PCRRF13001).

## References

1. B. Muthuraj, R. Deshmukh, V. Trivedi and P. K. Iyer, *ACS Appl Mater Interfaces*, 2014, **14**, 6562-6569.
2. R. Miao, L. Mu, H. Zhang, G. She, B. Zhou, H. Xu, P. Wang and W. Shi, *Nano Lett.*, 2014, **14**, 3124-3129.
3. C. Zong, K. Ai, G. Zhang, H. Li and L. Lu, *Anal. Chem.*, 2011, **83**, 3126-3132.
4. D. E. Kang, C. S. Lim, J. Y. Kim, E. S. Kim, H. J. Chun and B. R. Cho, *Anal. Chem.*, 2014, **86**, 5353-5359.
5. C. F. Monson, X. Cong, A. D. Robison, H. P. Pace, C. Liu, M. F. Poyton and P. S. Cremer, *J. Am. Chem. Soc.*, 2012, **134**, 7773-7779.
6. H. D. Song, I. Choi, S. Lee, Y. I. Yang, T. Kang and J. Yi, *Anal. Chem.*, 2013, **85**, 7980-7986.
7. J. Fan, P. Zhan, M. Hu, W. Sun, J. Tang, J. Wang, S. Sun, F. Song and X. Peng, *Org. Lett.*, 2013, **15**, 492-495.
8. J. Liu, C. Li and F. Li, *J. Mater. Chem.*, 2011, **21**, 7175-7181.
9. R. A. Løvstad, *BioMetals*, 2004, **17**, 111-113.
10. C. Vulpe, B. Levinson, S. Whitney, S. Packman and J. Gitschier, *Nat. Genet.*, 1993, **3**, 7-13.
11. K. J. Barnham, C. L. Masters and A. I. Bush, *Nat. Rev. Drug Discovery* 2004, **3**, 205-214.
12. R. Sheng, P. Wang, Y. Gao, Y. Wu, W. Liu, J. Ma, H. Li and S. Wu, *Org. Lett.*, 2008, **10**, 5015-5018.

- 1  
2  
3  
4  
5  
6  
7  
8  
9  
10  
11  
12  
13  
14  
15  
16  
17  
18  
19  
20  
21  
22  
23  
24  
25  
26  
27  
28  
29  
30  
31  
32  
33  
34  
35  
36  
37  
38  
39  
40  
41  
42  
43  
44  
45  
46  
47  
48  
49  
50  
51  
52  
53  
54  
55  
56  
57  
58  
59  
60
13. V. S. Jisha, A. J. Thomas and D. Ramaiah, *J. Org. Chem.* , 2009, **74**, 6667-6673.
14. S. Khatua, S. H. Choi, J. Lee, J. O. Huh, Y. Do and D. G. Churchill, *Inorg. Chem.* , 2009, **48**, 1799-1801.
15. M. Kumar, N. Kumar, V. Bhalla, P. R. Sharma and T. Kaur, *Org. Lett.* , 2011, **14**, 406-409.
16. P. G. Georgopoulos, A. Roy, M. J. Yonone Lioy, R. E. Opiekun and P. J. Lioy, *J. Toxicol. Env. Heal. B*, 2001, **4**, 341-394.
17. X. Liu, N. Zhang, T. Bing and D. Shangguan, *Anal. Chem.* , 2014, **4**, 2289-2296.
18. T. W. Lin and S. D. Huang, *Anal. Chem.* , 2001, **73**, 4319-4325.
19. N. Pourreza and R. Hoveizavi, *Anal. Chim. Acta* 2005, **549**, 124-128.
20. Y. Liu, P. Liang and L. Guo, *Talanta*, 2005, **68**, 25-30.
21. J. S. Becker, A. Matusch, C. Depboylu, J. Dobrowolska and M. Zoriy, *Anal. Chem.* , 2007, **79**, 6074-6080.
22. P. Jouhanneau, G. M. Raisbeck, F. Yiou, B. Lacour, H. Banide and T. B. Drueke, *Clin. Chem.* , 1997, **43**, 1023-1028.
23. J. V. Headley, D. B. Maxwell, C. Swyngedouw and J. R. Purdy, *J. AOAC Int.* , 1996, **79**, 117-123.
24. R. Y. Tsien, *Method. cell biol.*, 1989, **30**, 127-156.
25. D. J. Stephens and V. J. Allan, *Science*, 2003, **300**, 82-86.
26. M. Zhang, M. Yu, F. Li, M. Zhu, M. Li, Y. Gao, L. Li, Z. Liu, J. Zhang, D. Zhang, T. Yi and C. Huang, *J. Am. Chem. Soc.* , 2007, **129**, 10322-10323.
27. S. Kenmoku, Y. Urano, H. Kojima and T. Nagano, *J. Am. Chem. Soc.* , 2007, **129**, 7313-7318.
28. Y. Koide, Y. Urano, S. Kenmoku, H. Kojima and T. Nagano, *J. Am. Chem. Soc.* , 2007, **129**,

- 10324-10325.
29. L. Fabbrizzi, M. Licchelli, P. Pallavicini, A. Perotti and D. Sacchi, *Angew. Chem. Int. Ed.* , 1994, **33**, 1975-1977.
30. A. Torrado, G. K. Walkup and B. Imperiali, *J. Am. Chem. Soc.* , 1998, **120**, 609-610.
31. B. Valeur and I. Leray, *Coord. Chem. Rev.* , 2000, **205**, 3-40.
32. A. Zhu, Q. Qu, X. Shao, B. Kong and Y. Tian, *Angew. Chem. Int. Ed.* , 2012, **124**, 7297-7301.
33. A. K. Mahapatra, G. Hazra, N. K. Das and S. Goswami, *Sens. Actuators, B* 2011, **156**, 456-462.
34. X. Qi, E. J. Jun, L. Xu, S. J. Kim, J. S. Joong Hong, Y. J. Yoon and J. Yoon, *J. Org. Chem.* , 2006, **71**, 2881-2884.
35. V. Dujols, F. Ford and A. W. Czarnik, *J. Am. Chem. Soc.* , 1997, **119**, 7386-7387.
36. Y. Zhou, F. Wang, Y. Kim, S. J. Kim and J. Yoon, *Org. Lett.* , 2009, **11**, 4442-4445.
37. Y. Xiang, A. Tong, P. Jin and Y. Ju, *Org. Lett.* , 2006, **8**, 2863-2866.
38. M. Suresh, A. Shrivastav, S. Mishra, E. Suresh and A. Das, *Org. Lett.* , 2008, **10**, 3013-3016.
39. M. H. Lee, H. J. Kim, S. Yoon, N. Park and J. S. Kim, *Org. Lett.* , 2007, **10**, 213-216.
40. C. Wang and K. M. C. Wong, *Inorg. Chem.* , 2013, **52**, 13432-13441.
41. Y. Shiraishi, R. Miyamoto, X. Zhang and T. Hirai, *Org. Lett.* , 2007, **9**, 3921-3924.
42. Y. Zhao, X. B. Zhang, Z. X. Han, L. Qiao, C. Y. Li, L. X. Jian, G. L. Shen and R. Q. Yu, *Anal. Chem.* , 2009, **81**, 7022-7030.
43. J. Kuzelka, S. Mukhopadhyay, B. Spingler and S. J. Lippard, *Inorg. Chem.* , 2004, **43**, 1751-1761.
44. Y. Liu, X. Lv, Y. Zhao, J. Liu, Y. Q. Sun, P. Wang and W. Guo, *J. Mater. Chem.* , 2012, **22**,



- 1747-1750.
45. B. Zhao, J. Y. Wu, J. C. Tao, H. Z. Yuan and X. A. Mao, *Polyhedron*, 1996, **15**, 1197-1202.
46. P. F. Lee, C. T. Yang, D. Fan, J. J. Vittal and J. D. Ranford, *Polyhedron*, 2003, **22**, 2781-2786.
47. Z. H. Xu, W. Y. Guo, B. W. Su, X. K. Shen and F. L. Yang, *Acta. Crystallogr. Sect. E Struct. Rep. Online*, 2010, **66**, O1500-U2173.
48. Z. H. Xu, Y. L. Zhang, Y. R. Zhao and F. L. Yang, *Acta. Crystallogr. Sect. E Struct. Rep. Online*, 2010, **66**, O1504-U2218.
49. M. Yu, M. Shi, Z. Chen, F. Li, X. Li, Y. Gao, J. Xu, H. Yang, Z. Zhou and T. Yi, *Chem. Eur. J.*, 2008, **14**, 6892-6900.
50. M. Suresh, S. Mishra, S. K. Mishra, E. Suresh, A. K. Mandal, A. Shrivastav and A. Das, *Org. Lett.*, 2009, **11**, 2740-2743.
51. X. Zeng, L. Dong, C. Wu, L. Mu, S.F. Xue and Z. Tao, *Sens. Actuators, B* 2009, **141**, 506-510.
52. K. A. Connors, *Binding constants: the measurement of molecular complex stability*, Wiley New York, 1987.
53. M. I. Rodríguez-Cáceres, R. A. Agbaria, and I. M. Warner, *J. Fluoresc.*, 2005, **15**, 185-190.
54. X. Yu, A. J. Tong, P. Y. Jin, and Y. Ju, *Org. Lett.*, 2006, **8**, 2863-2866.

**Figure captions**

Figure 1 X-ray crystal structure of DFPP-RhB. Blue: N atom. Red: O atom.

Figure 2 UV/Vis (A) and fluorescence spectra (B) of DFPP-RhB (10  $\mu\text{M}$ ) upon addition of 200  $\mu\text{M}$  of different metal ions in ethanol, (C) and (D) show the photos of color and fluorescence changes of DFPP-RhB upon of various metal ions, respectively. ( $\lambda_{\text{ex}}$  = 520 nm, excitation slit: 10 nm, emission slit: 7.5 nm).

Figure 3 Absorption (A) and fluorescence (B) spectra of DFPP-RhB (10  $\mu\text{M}$ ) upon the addition of different amount of  $\text{Cu}^{2+}$  in ethanol. ( $\lambda_{\text{ex}}$  = 520 nm, excitation slit: 10 nm, emission slit: 7.5 nm).

Figure 4 The sensitivity test (detection limit) of DFPP-RhB towards  $\text{Cu}^{2+}$  using UV-Vis absorption technique (A) and fluorescence technique (B).

Figure 5 The probable recognition mechanism of DFPP-RhB towards  $\text{Cu}^{2+}$ .

Figure 6 The brightfield and confocal fluorescence images of HeLa cells. Brightfield, fluorescence and overlay images of living HeLa cells incubated with 10  $\mu\text{M}$  DFPP-RhB in DMSO/PBS (pH 7.4, 1:99, v/v) for 0.5 h at 37  $^{\circ}\text{C}$  (top three pictures). Brightfield, fluorescence and overlay images of living HeLa cells incubated with 10  $\mu\text{M}$   $\text{Cu}^{2+}$  in the grown media for 0.5 h at 37  $^{\circ}\text{C}$  and then incubated with 10  $\mu\text{M}$  DFPP-RhB in DMSO/PBS (pH 7.4, 1:99, v/v) for 0.5 h at 37  $^{\circ}\text{C}$  (bottom three pictures).

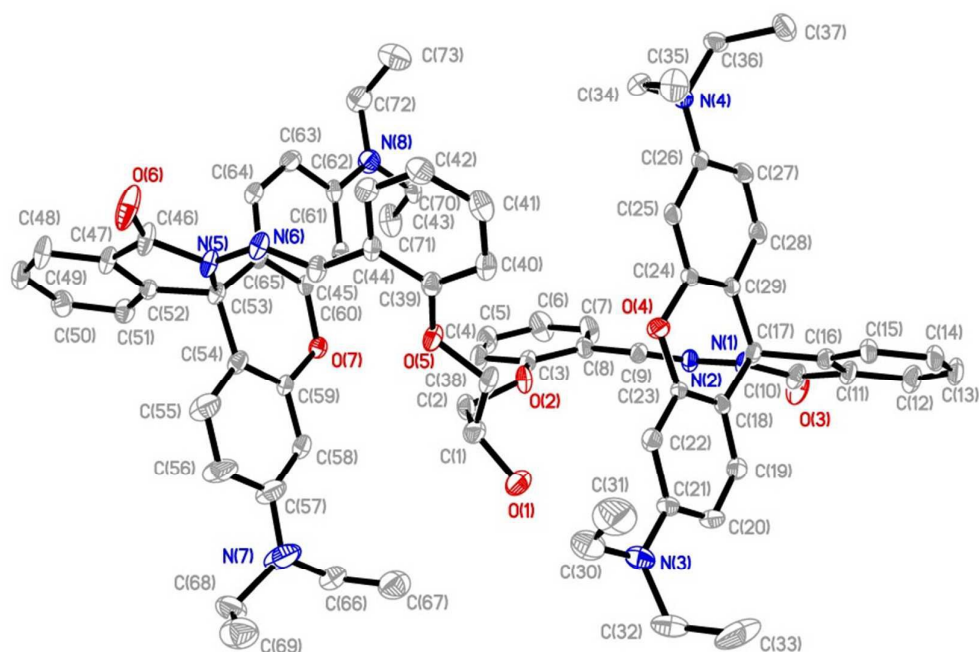


Fig. 1

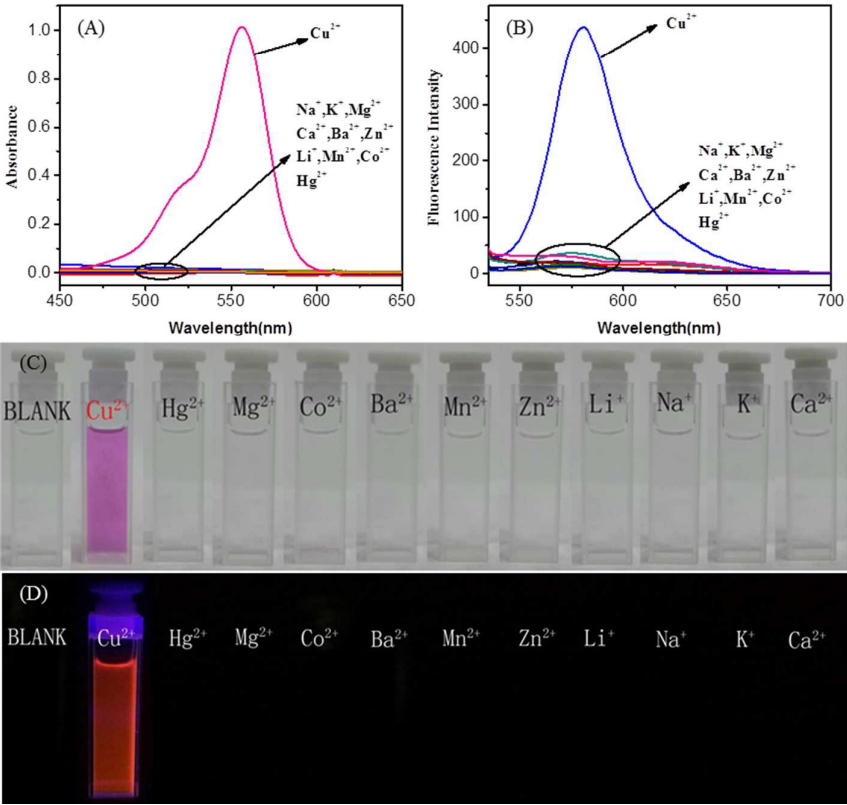


Fig. 2

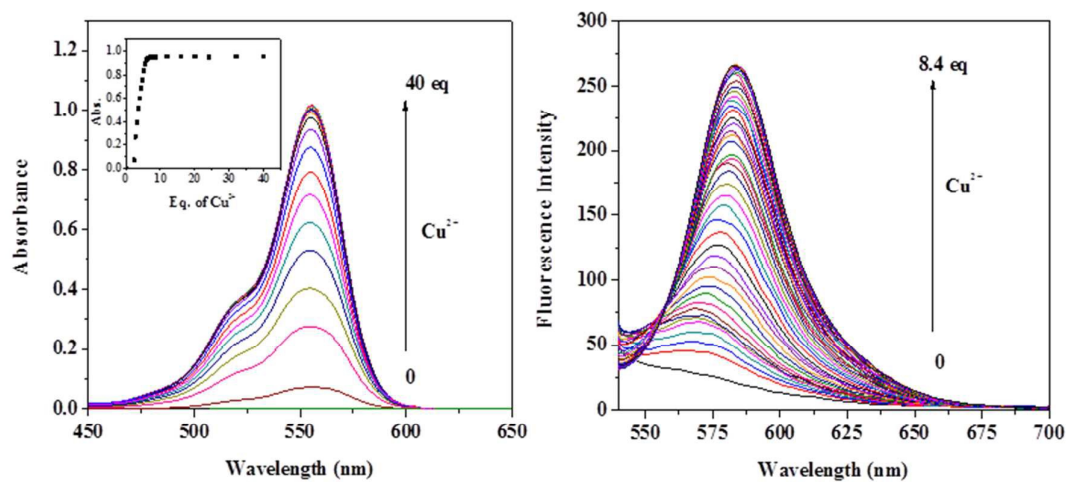


Fig. 3

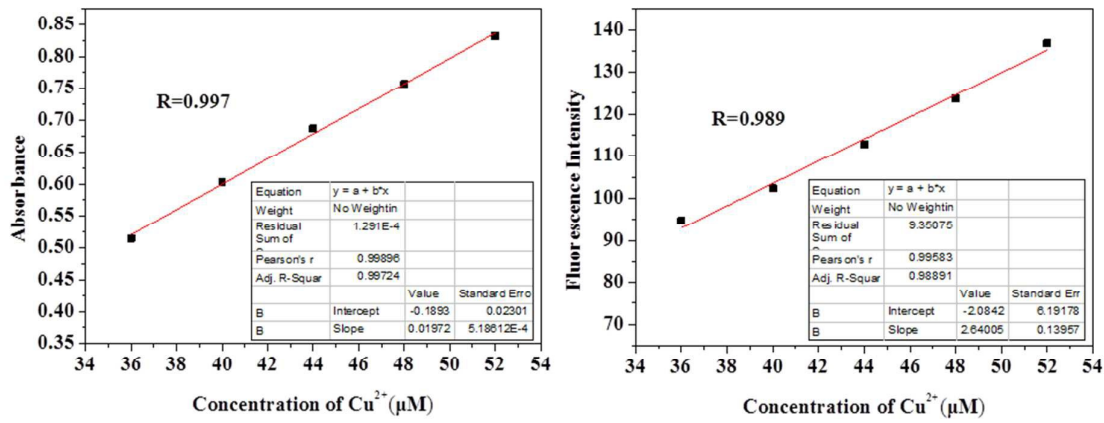


Fig. 4

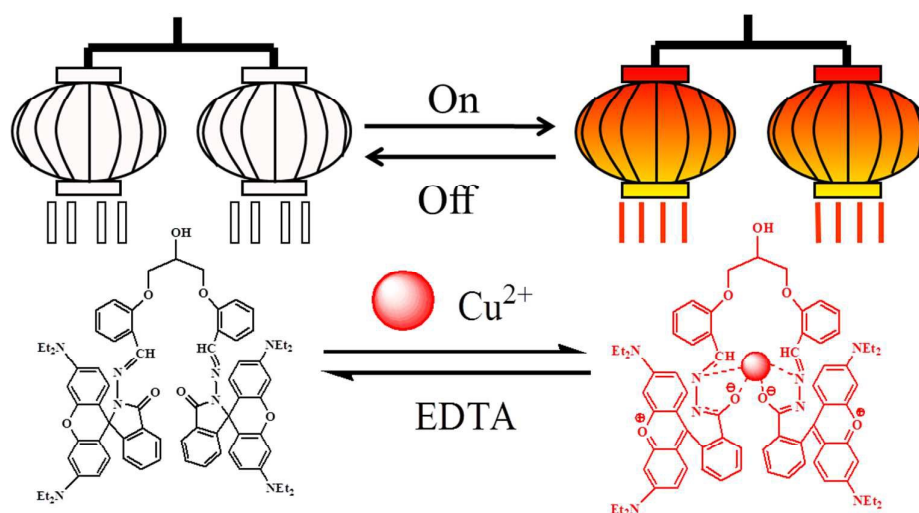
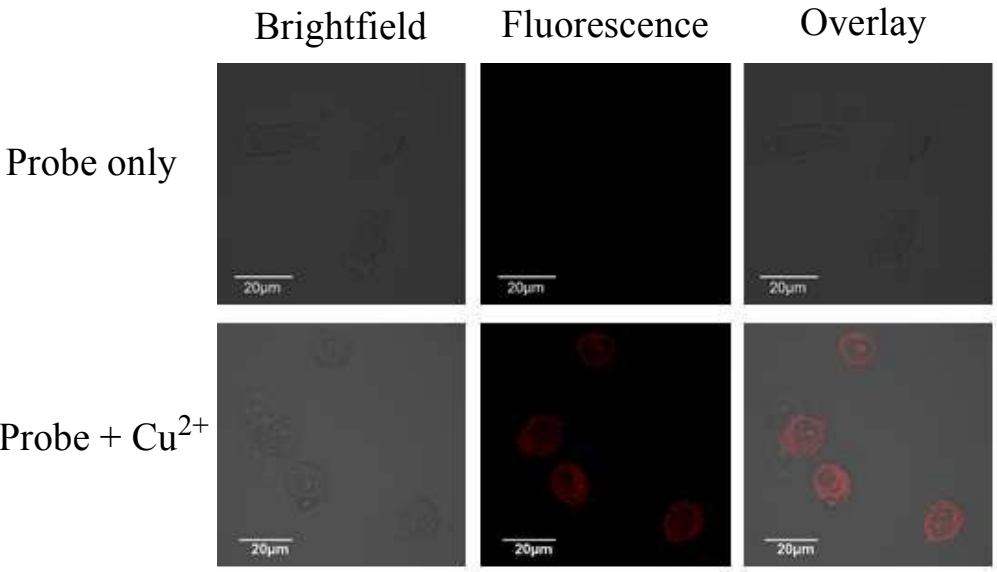


Fig. 5



Analytical Methods Accepted Manuscript

Fig. 6



## TOC

A novel fluorescent chemosensor containing two rhodamine B moieties per molecule with high symmetry structure was synthesized and characterized as an “off-on” fluorescent probe for the detection of copper ions. Living cell imaging experiment further demonstrates its value in bioimaging of intracellular  $\text{Cu}^{2+}$  by virtue of its nontoxic nature.

